analytical chemistry

Article

pubs.acs.org/ac

Analysis of Hydraulic Fracturing Flowback and Produced Waters Using Accurate Mass: Identification of Ethoxylated Surfactants

E. Michael Thurman,*[,†] Imma Ferrer,[†] Jens Blotevogel,[‡] and Thomas Borch*[,§,∥]

[†]Center for Environmental Mass Spectrometry, Department of Environmental Engineering, University of Colorado, Boulder, Colorado 80309, United States

[‡]Department of Civil and Environmental Engineering, [§]Department of Chemistry, and [∥]Department of Soil and Crop Sciences, Colorado State University, Fort Collins, Colorado 80523, United States

Supporting Information

ABSTRACT: Two series of ethylene oxide (EO) surfactants, polyethylene glycols (PEGs from EO3 to EO33) and linear alkyl ethoxylates (LAEs C-9 to C-15 with EO3−EO28), were identified in hydraulic fracturing flowback and produced water using a new application of the Kendrick mass defect and liquid chromatography/quadrupole-time-of-flight mass spectrometry. The Kendrick mass defect differentiates the proton, ammonium, and sodium adducts in both singly and doubly charged forms. A structural model of adduct formation is presented, and binding constants are calculated, which is based on a spherical cagelike conformation, where the central cation (NH_4^+ or Na^+) is coordinated with ether oxygens. A major purpose of the study was the identification of the ethylene oxide (EO) surfactants and the construction of a database with accurate masses and retention times in order to unravel the mass spectral complexity of surfactant mixtures used in hydraulic fracturing fluids. For example, over 500 accurate mass assignments are made in a few seconds of computer time, which then is used as a fingerprint chromatogram of the water samples. This technique is applied to a series of flowback and produced water samples to illustrate the usefulness of ethoxylate "fingerprinting", in a first application to monitor water quality that results from fluids used in hydraulic fracturing.

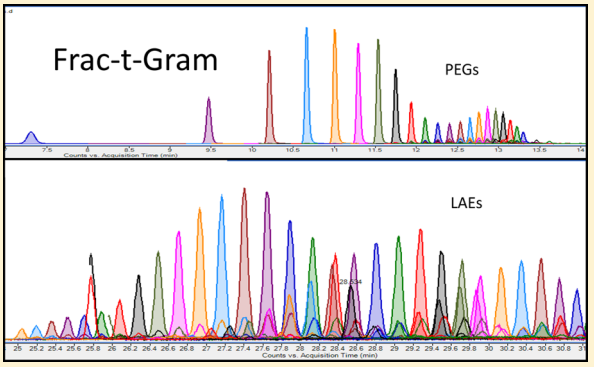

Hydraulic fracturing is a process of forcing aqueous fluids into gas- and oil-rich shales to enable or increase natural resource extraction. These fluids usually contain water and proppants (e.g., sand) as well as mixtures of chemical additives such as surfactants, biocides, friction reducers, and other compounds meant to help in the process of freeing the trapped gas.[1] The injected water (typically several million gallons per well), which partially returns from the hydraulic fracturing process, is called flowback water. The produced water, which is the native groundwater from the geologic formation that was fractured, and the flowback water have the potential to mix with nearby aquifers or surface water.

There are reports of groundwater contamination from hydraulic fracturing fluids most notably in Wyoming, New York, and Pennsylvania.[2] Because of the unknown health effects associated with hydraulic fracturing fluids, there is considerable public concern about groundwater contamination by this process.[3−5] A recent amendment to the Safe Drinking Water Act[6,7] has exempted hydraulic fracturing fluids from these EPA regulations.[7] Published lists of organic chemicals that are used in hydraulic fracturing exist;[8−12] however, there are no published research articles of indicator organic compounds that would be useful for tracking or "fingerprinting" groundwater or surface water impacted by hydraulic fracturing. Thus, there is a need to identify in detail the surfactants, biocides, and other compounds used in hydraulic fracturing fluids in order to provide a basis for monitoring, toxicology, and remediation studies.

The U.S. Environmental Protection Agency requires publication of chemical lists, which are available at several Web sites.[8−12] Furthermore, the State of Colorado, with over 7500 natural gas wells drilled for hydraulic fracturing since 2005, requires the publication of the hydraulic fracturing mixtures for each well.[11] However, the exact chemical details of the hydraulic fracturing mixture are poorly described, as it has proprietary value between various oil and gas chemical-supply companies. A common feature, though, of these lists is the use of nonionic, ethoxylated surfactants,[8−12] which are used to control the viscosity of the fracturing fluids, reduce surface tension, and assist fluid recovery.[13] They are listed generically as ethoxylated glycols and alcohol ethoxylates. Thus, these compounds are possible "fingerprinting" tracers of hydraulic fracturing fluids.

Received: June 11, 2014
Accepted: August 27, 2014
Published: August 27, 2014

Although polyethoxylated surfactants are commonly encountered in instrumental analysis by mass spectrometry, there are no published studies of ethoxylated surfactants (i.e., containing ethylene oxide units abbreviated EO) in groundwater or surface water, using a nontargeted accurate-mass approach. Furthermore, because the ethoxylated surfactants consist of a polymeric structure where the chain grows with the addition of ethylene glycol units, the use of the Kendrick mass defect[13] should be effective when used with accurate mass.

The Kendrick mass scale, which is based on CH_2 being equal to 14.000 00,[14] has been used effectively for hydrocarbons in order to find those compounds that are related by a growing chain of CH_2. The Kendrick mass scale converts the mass of CH_2 from 14.015 65 to 14.000 00.[15] Examples include several recent works using electrospray mass spectrometry dealing with petroleum crude oil,[15] produced waters containing naphthenic acids from oil sands,[16] and natural organic matter and humic substances.[17] There have not been applications of the Kendrick mass scale to ethylene glycol surfactants.

Thus, the unique objectives of this study were (1) to identify the chemical structures of the various families of the ethoxylated surfactants in water samples associated with hydraulic fracturing using a modified version of the Kendrick mass scale, (2) to develop a database of accurate masses with retention times for the families of ethoxylates, and, finally, (3) to apply this database to both flowback and produced water samples, for the validity of ethoxylates as indicators or unique "fingerprints" of groundwater mixing with hydraulic fracturing fluids.

EXPERIMENTAL SECTION

Sample Collection. In total, six flowback samples and six produced water samples were analyzed in this study. One produced water sample and three flowback samples were collected in Weld County, CO, by Tom Evans (ProTreat Technology Corp., Wheat Ridge, CO). They include two "slick frac" samples, i.e., low-viscosity (SF-1 and SF-2) and a produced water sample (SF-3), and a "gel frac" sample (GF-1) of higher viscosity due to addition of a gelling agent. All four samples are from hydraulically fractured extraction wells in the Denver-Julesburg Basin. Another flowback sample (YL-1) from the Denver-Julesburg basin was obtained by Yaal Lester from a different location and drilling company. The locations of the majority of wells are proprietary at this time. Two more flowback samples were obtained from Texas as part of the Barnett Shale (BS-1 and BS-2). Four produced water samples were obtained from Larry Zinkel of EPA from Nevada, Pennsylvania, and Louisiana (LZ-1−LZ-4). One produced water sample was obtained from James Rosenblum as a composite sample from Weld County (JR-1). All samples were treated as described below. Samples were stored in the dark and refrigerated. Samples were diluted 1:10 and filtered through surfactant-free 0.2 μm filters (Acrodisc) prior to analysis. Blank analyses were carried out on all filters and glassware used.

Ethoxylate and Hydraulic Fracturing Standards. The polyethylene standard, PEG 400, was obtained from Sigma-Aldrich and was used as a primary standard for the more-hydrophilic PEG compounds. Multi-Chem, a Halliburton Service (Houston, TX), generously supplied one commonly used surfactant mixture, which included both polyethylene glycol (PEG) and linear alkyl ethoxylate (LAE) sets of compounds. These surfactant mixtures were analyzed using the following ultrahigh pressure liquid chromatrography (UHPLC) method with liquid chromatography/quadrupole time-of-flight mass spectrometry (LC/Q-TOF/MS) analysis for further verification of retention times and accurate masses from the 12 samples analyzed in this study.

LC/Q-TOF/MS Analysis. The separation of the analytes was carried out using an UHPLC system consisting of thermostated autosampler, column compartment, and a binary pump (Agilent Series 1290, Agilent Technologies, Santa Clara, CA) equipped with a reverse phase C8 analytical column of 150 mm × 4.6 mm and a 3.5 μm particle size (Zorbax Eclipse XDB-C8). Column temperature was maintained at 25 °C. The injected sample volume was 20 μL. Mobile phases A and B were water with 0.1% formic acid and acetonitrile, respectively. The optimized chromatographic method held the initial mobile phase composition (10% B) constant for 5 min, followed by a linear gradient to 100% B after 30 min. The flow rate used was 0.6 mL/min. A 10 min postrun was used after each analysis. This UHPLC system was connected to an ultrahigh definition quadrupole time-of-flight mass spectrometer model 6540 Agilent (Agilent Technologies, Santa Clara, CA) equipped with electrospray Jet Stream Technology, operating in positive ion mode, using the following operation parameters: capillary voltage, 4000 V; nebulizer pressure, 45 psig; drying gas, 10 L/min; gas temperature, 250 °C; sheath gas flow, 11 L/min; sheath gas temperature, 350 °C; nozzle voltage, 1000 V, fragmentor voltage, 190 V; skimmer voltage, 45 V; octopole RF, 750 V. LC/MS accurate mass spectra were recorded across the range 50−1000 m/z at 2 GHz. The data recorded were processed with MassHunter software (version 6.1). Accurate mass measurements of each peak from the total ion chromatograms were obtained by means of an automated calibrant delivery system using a low flow of a calibrating solution (calibrant solution A, Agilent Technologies, Inc.), which contains the internal reference masses (purine m/z 121.0509 and HP-921 at m/z 922.0098). The instrument provided a typical mass resolving power of 30 000 at m/z 1522.

Database Application. A comma separated value (csv) Excel file was created with the neutral mass of the PEGs and LAE surfactants as a function of their ethylene oxide chain length. The retention time and accurate masses were then entered into the csv Excel file for use with the database function of the software, called "Find by Formula". The "Find by Formula" tab is used and the csv file is searched using the command, "Find Compounds by Formula". The software will display the hits along with the mass accuracy and intensities. Both singly and doubly charged species are displayed.

Quantum Chemical Calculations. Density functional theory (DFT) calculations were conducted via Gaussian 09 to describe the nature of the complexation for PEG with the ammonium or sodium cation, respectively, and to estimate their binding constants. All calculations were performed at the B3LYP/6-311G(d,p) level of theory, which has been shown to produce accurate geometries, bond distances, and conformational energies.[18] The integral equation formalism polarizable continuum model (IEFPCM) was applied to account for solvent effects. The dielectric constants used to describe the respective acetonitrile/water mixtures at the time of analyte elution were derived from Gagliardi et al.,[19] i.e., ε = 73.1 for PEG EO-9 (18% ACN), ε = 73.8 for PEG EO-8 (16% ACN), and ε = 74.5 for PEG EO-7 (14% ACN). To locate the lowest-energy conformations, ground-state energies were determined as a function of the number of PEG-bound oxygen atoms interacting with the cation. Binding constants K were calculated

dx.doi.org/10.1021/ac502163k | Anal. Chem. 2014, 86, 9653−9661

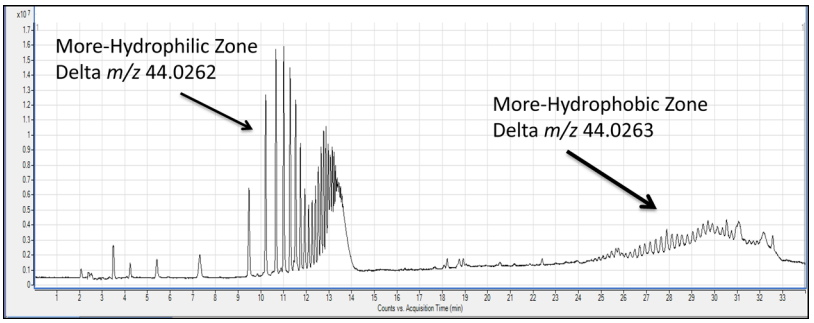

Figure 1. UHPLC LC/Q-TOF/MS chromatogram in positive ion mode of SF-1 flowback sample from the Denver-Julesburg Basin. The chromatogram shows a more-hydrophilic zone at 3.5−14 min and a more-hydrophobic zone at 24−30 min. The mass difference between each peak in the series was 44.0262 and 44.0263 (exact calculated mass of 44.0262), respectively, which is an average of 1- ppm mass accuracy for the neutral difference.

Table 1. Putative Identifications of PEG Adducts Using the Kendrick Masses and Mass Defects for a Suite of Major Ions Found in SF-1 from the Denver-Julesburg Basin, Based on a Scaling Factor of Ethylene Oxide Equaling 44.0000/44.0262 Mass Units, i.e., a Scaling Multiplier of 0.999 404 559

time (min)	measured mass (m/z)	Kendrick mass	Kendrick mass defect	putative formula	putative identification	calculated exact mass(m/z)	error (ppm)
3.5	173.0784	172.975	0.975	$C_6H_{14}O_4Na^+$	PEG-EO3 Na adduct	173.0784	0.0
4.2	217.1042	216.975	0.975	$C_8H_{18}O_5Na^+$	PEG-EO4 Na adduct	217.1046	2.0
5.4	261.1304	260.975	0.975	$C_{10}H_{22}O_6Na^+$	PEG-EO5 Na adduct	261.1309	2.0
7.3	305.1569	304.975	0.975	$C_{12}H_{26}O_7Na^+$	PEG-EO6 Na adduct	305.1571	0.7
9.5	349.1833	348.975	0.975	$C_{14}H_{30}O_8Na^+$	PEG-EO7 Na adduct	349.1833	0.0
10.2	393.2092	392.975	0.975	$C_{16}H_{34}O_9Na^+$	PEG-EO8 Na adduct	393.2095	0.8
10.7	432.2802	432.023	0.023	$C_{18}H_{38}O_{10}NH_4^+$	PEG-EO9 NH_4 adduct	432.2803	0.2
11.0	476.3066	476.023	0.023	$C_{20}H_{42}O_{11}NH_4^+$	PEG-EO10 NH_4 adduct	476.3065	0.2
11.3	520.3324	520.023	0.023	$C_{22}H_{46}O_{12}NH_4^+$	PEG-EO11 NH_4 adduct	520.3328	0.8
11.5	564.3585	564.022	0.022	$C_{24}H_{50}O_{13}NH_4^+$	PEG-EO12 NH_4 adduct	564.3590	0.9
11.7	608.3856	608.023	0.023	$C_{26}H_{54}O_{14}NH_4^+$	PEG-EO13 NH_4 adduct	608.3852	0.7
11.9	652.4113	652.023	0.023	$C_{28}H_{58}O_{15}NH_4^+$	PEG-EO14 NH_4 adduct	652.4114	0.2

using $\Delta G^0 = -2.303RT \log K$, where ΔG^0 is the standard Gibbs free energy change for the complexation of PEG and the respective cation, R is the gas constant, and T is the temperature. All potential energy minima were verified by frequency calculations (i.e., no imaginary frequencies).

RESULTS AND DISCUSSION

Identification of Polyethylene Glycol Ethoxylates using a Modified Kendrick Mass Scale. Figure 1 shows the UHPLC LC/Q-TOF/MS chromatogram in positive ion electrospray mode for the flowback sample SF-1 from the Denver-Julesburg Basin. Note that the chromatogram shows two distinct zones. First is the early eluting peaks in the more polar region of the chromatogram at a retention time of 3.5−14 min (referred to herein as the "more hydrophilic" peaks), and the second region from 24 to 33 min represents a more nonpolar region (referred to herein as the "more hydrophobic" peaks) of the chromatogram. These distinct zones are based on their retention times within this slow gradient profile. The hydrophilic peaks eluted at 10−40% acetonitrile, and the hydrophobic peaks eluted at 70−95% acetonitrile. The series of peaks in both regions are separated by 44 mass units (Table S1, Supporting Information), which suggests an ethoxylated structure consisting of (CH_2−CH_2−O). This hypothesis is tested by the accurate mass data in Table S1 (Supporting Information), which shows that the mass difference for the first 10 peaks in zone 1 (the more hydrophilic region of the chromatogram from 3.5 to 11.9 min) varies from 44.0258 to 44.0264, with an average mass of 44.0262, which is consistent with an ethoxylated structure (calculated exact mass of 44.0262).

A similar result was also observed for the second zone between 26.3 and 29.3 min (Table S1, Supporting Information), with the first 10 chromatographic peaks separated by an average accurate mass of 44.0263. Thus, the measured accurate masses support the hypothesis that each region is a homologous series of ethoxylates differing in the number of (CH_2−CH_2−O) units. These two series represented the majority of unknown peaks occurring in the chromatogram of Figure 1, which indicate that they are major components in this positive ion electrospray chromatogram, based upon ion formation. Thus, the Kendrick mass scale was applied to each of these two series, which were thought to contain the ethoxylate structure.

The Kendrick mass scale, based on CH_2 equaling exactly 14.0000, was developed by Kendrick in 1963[14] to better separate and understand a homologous series of hydrocarbons that were separated by a methylene group, $-CH_2$. It has been used on other series, such as lipids[20] and naphthenic acids from produced water samples from oil sands,[16] but has not been applied to ethoxylated homologues, based on our literature search. Thus, the application here is a modified Kendrick mass scale, since the additive group is an ethylene oxide unit ($-CH_2CH_2O-$) rather than a methylene unit. The general concept of applying the Kendrick mass scale is that if two or more compounds have the same chemical backbone, (such as

dx.doi.org/10.1021/ac502163k | Anal. Chem. 2014, 86, 9653−9661

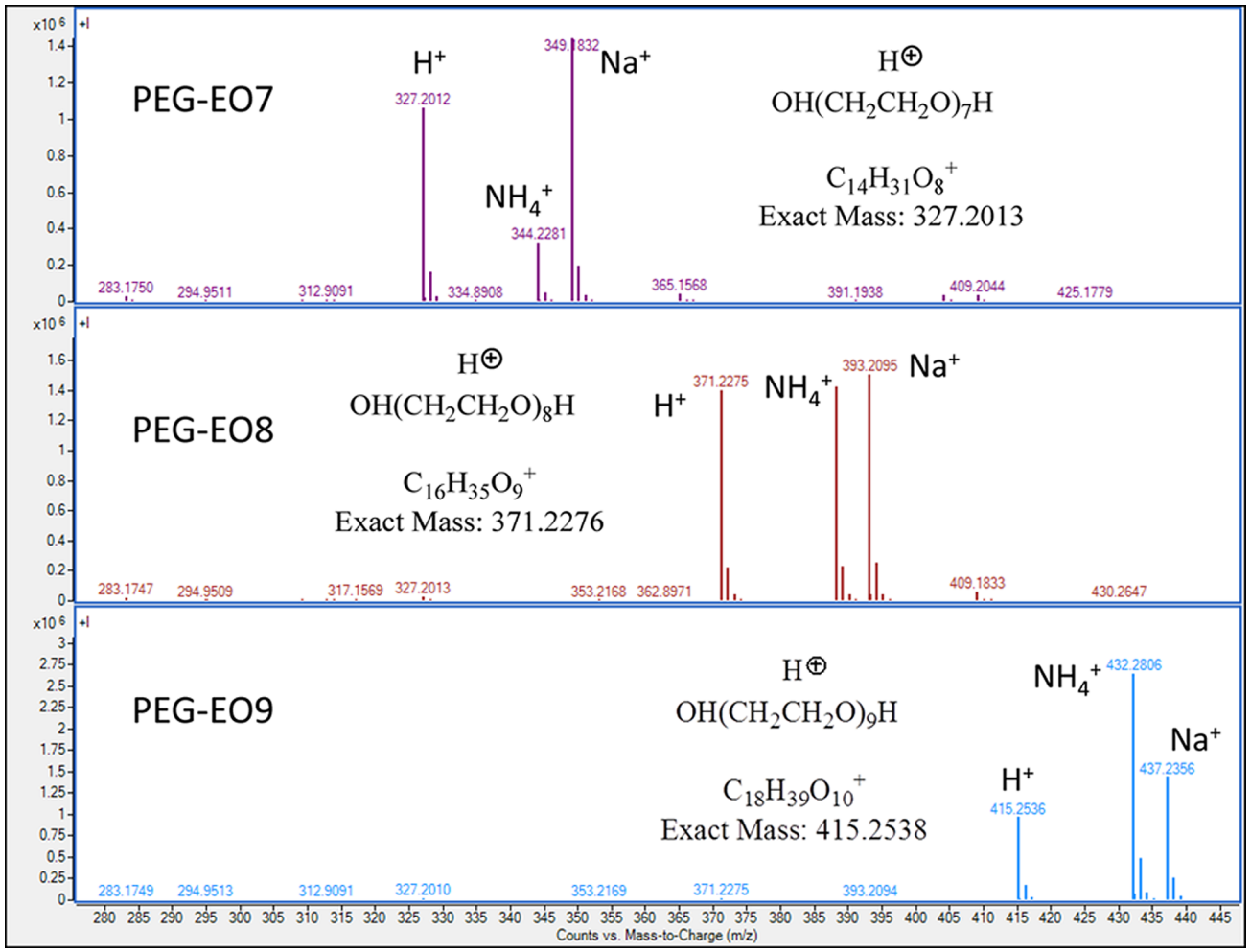

Figure 2. Mass spectra of putative structures for PEG-EO7, -EO8, and -EO9 with calculated exact masses showing accuracies of 0.3−0.5 ppm for the MH^+ for sample SF-1. Overall mass accuracies are less than 1 ppm.

R−CH_2CH_2OH), but are differing by one or more ethylene oxide units, then they will have the same Kendrick mass defect. Where the mass defect is the difference between the nominal Kendrick mass and the exact Kendrick mass.[15]

The Kendrick mass scaling factor is calculated as the ratio of the nominal mass of CH_2CH_2O (i.e., 44.0000) to the exact mass of the ethylene glycol unit (44.0262), which gives a value of 0.999 404 559 (i.e., 44.0000/44.0262 = 0.999 404 559). This factor is then multiplied with the accurate masses found in the total ion chromatogram (retention times of 3.5−14 min; more hydrophilic zone) in Figure 1 to generate the Kendrick mass table. When this is done, all the masses that are related by an increasing unit of the ethoxylate group (Kendrick mass of 44.0000) will have exactly the same Kendrick mass defect within the error of an accurate mass measurement, which for this study was typically ±0.0005 mass units. The Kendrick mass values for peaks from 3.5 to 11.9 min are shown in Table 1 for sample SF-1.

Table 1 shows that the measured masses of the respective major ions had mass defects ranging from 0.0784 (peak at 3.5 min) to 0.4113 (peak at 11.9 min). However, after multiplying by the appropriate Kendrick mass scaling factor of ethoxylate of 0.999 404 559, only two Kendrick mass defects (i.e., 0.975 and 0.023) were found for this suite of 12 ions. The first set (measured masses of m/z 173.0784−393.2092) gave the putative formulas of polyethylene glycol ethoxylate-3 (PEG-EO3) through PEG-EO8 as the respective sodium adduct of various polymers of PEG, where EO stands for an ethylene oxide unit. Overall mass accuracies varied from 0.0 to 2.0 ppm with a median value of 0.7 ppm (Table 1) for these various PEG adducts.

The second set of measured masses of m/z 432.2802−652.4113 in Table 1 gave the putative structures of the respective ammonium adduct of the PEG-EO9−PEG-EO14, also with an increase of one ethoxylate unit per compound. The data in Table 1 represent the largest intensity ion of each peak in the chromatogram shown in Figure 1, since multiple adducts occurred (Figure 2). For example, Figure 2 shows the accurate mass measurements of the proton, ammonium, and sodium PEG adducts from PEG-EO7 to PEG-EO9 from this same chromatogram (Figure 1). Their accurate masses varied from 0.3 to 0.5 ppm for the MH^+ ion.

The putative structures for each of the hydrophilic PEGs (retention times from 3.5 to 14 min) present in the sample were verified next by the analysis of a PEG standard (PEG-400 for PEG-EO3−PEG-EO14), which matched the retention times and accurate masses in Table 1. The usefulness of the Kendrick mass scale is that it is only necessary to determine the structure of one of the PEG surfactants, and the remaining structures with the same Kendrick mass defect represent the addition of one or more ethylene oxide units. This is even more valuable for ethoxylate analysis, where standards may not be

dx.doi.org/10.1021/ac502163k | Anal. Chem. 2014, 86, 9653−9661

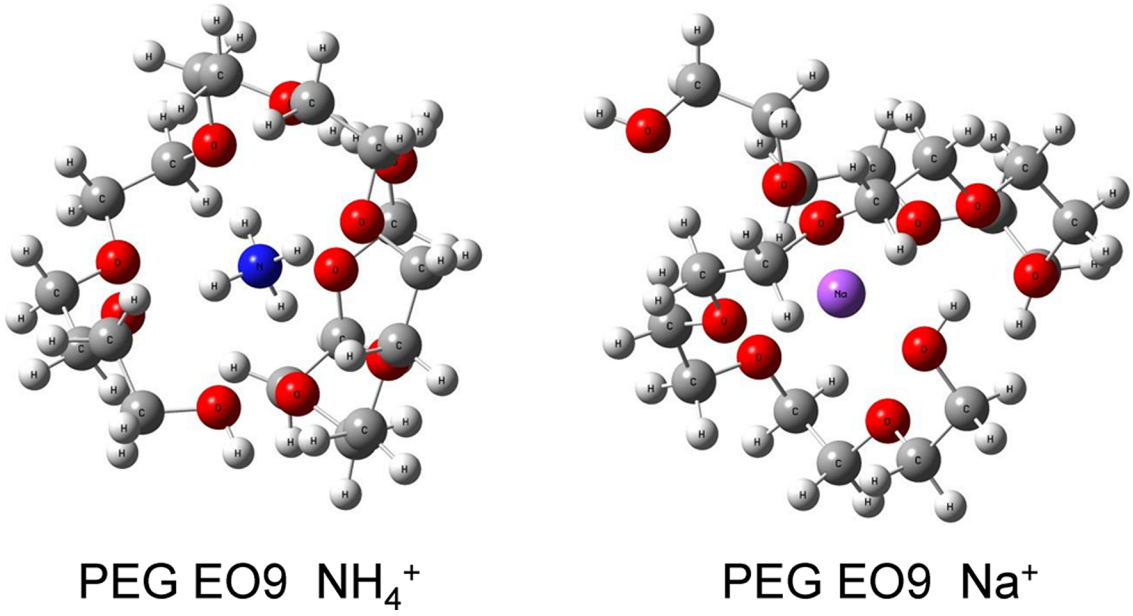

Figure 3. Lowest-energy conformations of the PEG-EO9 ammonium complex (left) and the PEG-EO9 sodium complex (right) calculated at the IEFPCM/B3LYP/6-311G(d,p) level of theory. The confirmations indicate a spherical or ball shape for both the ammonium and sodium adducts.

available, such as for the hydraulic fracturing fluids and flowback waters. Surprisingly few papers have been published on the environmental mass spectrometry of PEGs[21−23] because they are considered nuisance compounds in mass spectrometry as contaminants from filters and glassware. The value, though, of a thorough understanding of PEG fragmentation and adduct formation will be quite useful in a following section that deals with the more-hydrophobic EO surfactants.

Quantum Calculations of Adduct Formation. It is interesting to note that as the chain length increased from EO7 to EO9, the adduct of PEG changed from a predominantly sodium adduct to a predominantly ammonium adduct (compare the intensity of the NH_4^+ mass spectra in Figure 2 from m/z 344.2281 to 432.2806), which suggests that there are subtle changes in the cavity of the ammonium−ethoxylate ion that better stabilizes the NH_4^+ adduct, changing from a sodium-preferred adduct to an ammonium-preferred adduct. For EO9 the ammonium adduct becomes the major adduct, and at EO10, the ammonium adduct accounts for ∼70% of the total ion chromatogram and remains constant with the increasing number of ethoxylate units. Thus, density functional theory (DFT) calculations were carried out to gain insight into binding constants between both the sodium and ammonium PEG adducts and why there is a preference at EO9 for the ammonium adduct. Furthermore, the concentrations of both ammonium and sodium were measured in the mobile phases, reagents, and samples in order to better explain adduct formation.

The concentration of ammonium and sodium entering the mass spectrometer was 5 ± 1 and 276 ± 30 ppb, respectively (Table S2 in the Supporting Information gives ammonium and sodium concentrations for reagents, mobile phase, and sample). The SF-1 sample contained 50 ppm sodium and less than 1 ppb ammonium (Table S2, Supporting Information), which was diluted by mobile phase after injection of 10 μL into the mobile phase, and contributed to less than 10% of the total sodium at the mass spectrometer. Thus, the molar ratio of sodium to ammonium in the ion source was approximately 40:1 ± 10:1 when the PEG-EO9 elutes from the column.

Next the DFT calculations showed that, for both ammonium- and sodium-complexed PEG-EO9, the complexes become more stable with an increasing number of PEG-bound oxygen atoms oriented toward and thus interacting with the cation (see data in Tables S3 and S4 in the Supporting Information). In its respective lowest energy conformation shown in Figure 3, the linear PEG molecule is coiled up around the central ammonium or sodium ion, minimizing the average N−O distance to 3.14 Å (with a minimum N−O distance of 2.87 Å), and minimizing the average Na−O distance to 3.00 Å (with a minimum Na−O distance of 2.44 Å). For details, see Tables S3 and S4 in the Supporting Information. This spherical cagelike conformation, where the central cation is coordinated with the ether oxygens, has previously been observed in both experimental and theoretical studies of different, related, alkali ion-cationized polyethers in the gas phase.[24]

The calculated binding constants for different EO chains (Table S5 in the Supporting Information) revealed that the complexation of PEG-EO9 with ammonium (log K = 9.7) is more favorable than with sodium (log K = 7.9) by a factor of 63. Thus, although the sodium concentration is approximately 40 times greater than ammonium, the stronger complexation of PEG with ammonium explains why the ammonium adduct is the major observed ion of the mass spectrum for PEG-EO9 (Figure 2). For PEG-EO8, the ammonium adduct (log K = 11.1) is still determined to be more favorable than the sodium adduct (log K = 10.0) by approximately 13 times. The slight preference of the PEG-EO8 sodium adduct observed in the mass spectrum of Figure 2 again can be rationalized by the higher concentration of sodium in the mobile phase. However, with decreasing PEG chain length, the thermodynamic favorability shifts toward the sodium adduct (see Table S5, Supporting Information). For PEG-EO7, the sodium adduct (log K = 12.2) is then estimated to be the more favorable than the ammonium adduct (log K = 11.8), in agreement with the observed mass spectrum (Figure 2). The probable reason for

dx.doi.org/10.1021/ac502163k | Anal. Chem. 2014, 86, 9653−9661

Table 2. Doubly Charged PEGs Showing Both H^+ and NH_4^+ Adducts at EO Lengths of 17−19 and Then Double NH_4^+ Adducts from PEG-EO20 to PEG-EO26

time (min)	measured mass (m/z)	Kendrick mass $(M + H + NH_4)^{2+}$	Kendrick mass defect	molecular mass of neutral PEG	putative identification of doubly charged ion
12.4	392.7492	392.515	0.515	766.4562	$[H + NH_4]^{2+}$ PEG-EO17 adduct
12.5	414.7622	414.515	0.515	810.4824	$[H + NH_4]^{2+}$ PEG-EO18 adduct
12.6	436.7751	436.515	0.515	854.5086	$[H + NH_4]^{2+}$ PEG-EO19 adduct
12.7	467.3014	467.023	0.023	898.5349	$[NH_4]^{2+}$ PEG-EO20 adduct
12.8	489.3147	489.023	0.023	942.5611	$[NH_4]^{2+}$ PEG-EO21 adduct
12.9	511.3278	511.023	0.023	986.5873	$[NH_4]^{2+}$ PEG-EO22 adduct
13.0	533.3409	533.023	0.023	1030.6135	$[NH_4]^{2+}$ PEG-EO23 adduct
13.1	555.3540	555.023	0.023	1074.6397	$[NH_4]^{2+}$ PEG-EO24 adduct
13.2	577.3672	577.023	0.023	1118.6659	$[NH_4]^{2+}$ PEG-EO25 adduct
13.3	599.3808	599.024	0.024	1162.6921	$[NH_4]^{2+}$ PEG-EO26 adduct

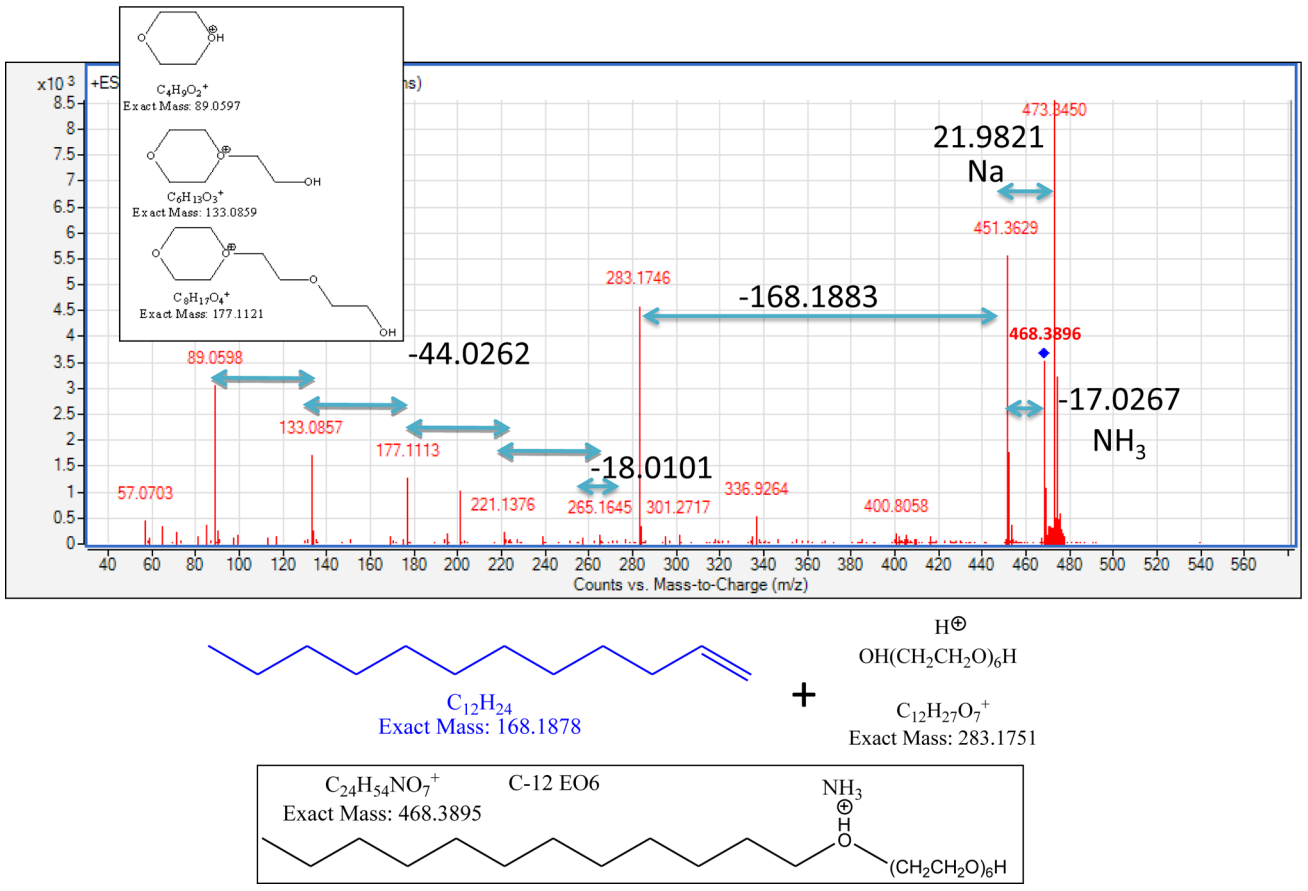

Figure 4. MS−MS of m/z 468 with a putative identification of C-12 EO6 NH_4^+ for sample SF-1. Mass accuracies are 0.2 ppm for NH_4^+ adduct and 1.5 ppm for the major fragment ion at m/z 283.1746.

the observed shift in thermodynamic favorability lies in the different ionic radii of the two cations. Because ammonium is larger (0.143 Å) than sodium (0.102 Å), it may interact with more oxygen atoms, thus becoming more favorable with increasing PEG chain length relative to the sodium adduct.[24]

Kendrick Mass Scale and Multiply Charged Adducts. The Kendrick mass scale was also applied to doubly charged adducts of the PEGs as the ethoxylate chain length increased greater than EO17 (Table 2). These multiply charged adducts likely form due to the growing chain length being able to form multiple cation-harboring regions with a cagelike structure. For example, Table 2 shows the data for PEGs with EO chain lengths of EO17−EO26. PEG-EO17−PEG-EO19 were mainly doubly charged PEGs with mixed adducts of proton and ammonium (Table 2), whereas PEG-EO20−PEG-EO26 consisted of the PEG doubly charged by two ammonium groups as the major component. The mass spectra for these compounds increased in complexity as they consisted of a variety of singly and doubly charged adducts, as shown in Figure S1 (Supporting Information). The mass spectrum in Figure S1 (Supporting Information) serves as an example of the six types of adducts forming for doubly charged PEGs, which are basically combinations of the three adducting ions, proton, ammonium, and sodium. The use of the Kendrick masses facilitated finding and identifying these mixed adducted polymeric species for the doubly charged PEGs (Table 2 and

dx.doi.org/10.1021/ac502163k | Anal. Chem. 2014, 86, 9653−9661

Table 3. Analysis of Flowback and Produced Water Samples for PEGs and LAEs[a]

sample name	sample type and location	presence of polyethoxylates (PEGs)	presence of polyethoxylates bimodal (PEGSs)	presence of linear alkyl ethoxylates (LAEs)
SF-1	flowback, CO	yes	yes	yes
SF-2	flowback, CO	yes	none	yes
SF-3	produced, CO	yes	none	none
GF-1	flowback, CO	yes	yes	none
YL-1	flowback, CO	trace	none	yes
BS-1	flowback, TX	none	none	trace
BS-2	flowback, TX	none	none	trace
LZ-1	produced, LA	none	none	none
LZ-2	produced, NV	trace	none	none
LZ-3	produced, NV	none	none	none
LZ-4	produced, PA	trace	none	none
JR-1	produced, CO	yes	yes	trace

[a]"Yes" indicates major components, "trace" is low but detectable, and "none" is no detection.

Figure S1, Supporting Information). The doubly charged mixed adducts shown in Figure S1 (Supporting Information) are a new finding and are not available in commercial software. Thus, these adducts were identified using manual application of the Kendrick mass scale. The authors are in the process of incorporating these findings into the Agilent MassHunter software in collaboration with the manufacturer.

With these identifications on hand using the Kendrick masses, it was possible to build an accurate mass database (ethoxylate database) of these PEG ions and structures (PEG-EO3−PEG-EO33), which can then be used for identification of PEGs in waters associated with hydraulic fracturing. The database of PEG adducts with their accurate masses and formulas can be quickly applied to a sample for their identification using both accurate mass and retention times, which will be illustrated in the last section under sample analysis for the 12 samples studied thus far.

Identification of Linear Alkyl Ethoxylates. The more-hydrophobic zone of the chromatogram was examined in similar fashion as the more-hydrophilic zone with determination of the differences in accurate mass between homologues (Table S6, Supporting Information). Between 26.3 and 27.9 min the accurate mass changes on average by 44.0263, again implying that this is a homologous series of (CH_2CH_2O). However, this time the masses are decreasing with increasing retention time, as compared to the PEGs that are increasing in mass with increasing retention time (compare Tables S1 and S6, Supporting Information). The same fact is seen in the homologous series from 28.1 to 29.3 min in Table S6 (Supporting Information), where masses decrease with increasing retention time, with an average mass difference of 44.0263 between homologues. The fact that the masses are less as retention time increases suggests that hydrophobicity is increasing with the decreasing chain length of the ethoxylate. The simplest explanation for these results is that this surfactant series consists of a hydrophobic group and that the ethoxylate chain is the (relatively) hydrophilic portion of the surfactant. As the ethoxylate groups are removed from the molecule and the mass decreases, the hydrophobicity increases and this is detected as a longer retention time on the C-8 column of the UHPLC. This hypothesis will be tested by MS−MS analysis.

Thus, Figure 4 shows the MS−MS spectrum for sample SF-1. There is the MH^+ ion at a nominal mass of m/z 451, the ammonium adduct at m/z 468, and the sodium adduct at m/z 473. The accurate mass differences among the adducts are 17.0267 ($MNH_4^+ - MH^+$) and 21.9821 ($MNa^+ - MH^+$), which indicate that there are ammonium and sodium adducts and the mass at m/z 451.3629 is the MH^+. The ammonium adduct was chosen for MS−MS analysis because it gave the largest peak at m/z 468 prior to MS−MS analysis.

The first loss is of NH_3 to yield the m/z 451 ion (Figure 4), which then lost 168.1883 mass units to give the m/z 283.1746 ion. The loss of 168.1883 was calculated from its accurate mass to be an aliphatic chain of 12 carbon atoms. Note the calculated exact mass loss of 168.1878 versus the measured loss of 168.1883 in Figure 4 (2.9 ppm mass accuracy). The simplest structure that matches this loss is the aliphatic C-12 chain, consistent with a simple aliphatic ethoxy structure, also called linear alkylethoxylates or LAEs.[22] The m/z 283.1746 ion then undergoes a water loss to give the m/z 265.1645 ion followed by a series of losses of 44 mass units to give the diagnostic ions of the PEG structure, m/z 89, 133, and 177.[21]

The accurate mass ion of m/z 283.1746 is the accurate mass for the PEG-EO6, which has a calculated mass of m/z 283.1751 (Figure 4). The MS−MS analysis of PEG-EO6 gives a fragmentation pattern similar to that shown in Figure 4 (data not shown). Thus, the conclusion is that the final putative structure is a C-12 linear alkyl ethoxylate of EO6. Again the application of the Kendrick masses allows one to assign putative structures to the remaining ions in Table S6 (Supporting Information), from C-12 EO6 to C-12 EO13. The reverse elution order is consistent with the fact that, as the EO chain increases, the surfactant becomes more hydrophilic and elutes earlier in the chromatographic run. The second group in Table S6 (Supporting Information) consists of C-13 EOs on the basis of their Kendrick masses. Thus, again the usefulness of the Kendrick mass scale is shown here, in that now, when one structure has been putatively identified, one can then extrapolate all of the remaining structures for the peaks that contain the same Kendrick mass defect. The MS−MS analysis was also repeated for the MH^+ ion at m/z 451.3629 (Figure 4), which gave a similar fragmentation pattern to that of the ammonium adduct, as expected. Again, the value of a thorough understanding of adduct formation is the critical and innovative step in identification of these surfactant mixtures, which is based on understanding PEG ion and adduct formation. The data from Table S6 (Supporting Information) has also been added to the database such that the majority of the chromatographic peaks shown in Figure 1 (sample SF-1) are

dx.doi.org/10.1021/ac502163k | Anal. Chem. 2014, 86, 9653−9661

incorporated into the database for further sample analysis, as shown in the following section.

Analysis of Flowback and Produced Water Samples. The method shown here, using the Kendrick mass scale and PEG-EO and LAE-EO databases, has been applied to six flowback water samples and six produced water samples (Table 3). Table 3 displays the detections for each of the samples for both the PEGs and LAEs. Four of the six flowback samples had major detections of PEGs (SF-1−SF-3 and GF-1). Two of the flowback samples also showed a bimodal distribution of PEGs (SF-1 and GF-1). The PEGs have the most abundant species at PEG-EO-9 and again at PEG-EO-21. The use of the longer chain PEGs may be used as friction reducers or for viscosity optimization[13] and may be unique to the hydraulic fracturing fluids. Three of the six flowback samples also had major detections of the LAEs (SF-1, SF-2, and YL-1). Trace levels of the LAEs were found in two of the flowback samples (BS-1 and BS-2). Thus, in general, the flowback samples contained major detections of both PEGs and/or LAEs.

In contrast, the produced water samples gave less detections of either PEGs or LAEs. For example, only two of the six produced water samples contained major detections of PEGs (SF-3 and JR-1) and two more had trace detections of PEGs (LZ-2 and LZ-4). Only one produced water sample showed the bimodal distribution of PEGs (JR-1). Five of the six produced water samples showed no detections of LAEs (SF-3, LZ-1, LZ-2, LZ-3, and LZ-4), and one sample had a trace detection of LAEs (JR-1). Although it is premature to establish trends with only 12 samples, it does appear that flowback water samples have greater detections and higher levels of PEGs and LAEs than produced waters. This conclusion seems logical given that produced water samples should not contain EO surfactants, since they arise from the geologic formation. Because flowback water is injected into the formation during hydraulic fracturing, there is not a clear boundary between the injected water and the native groundwater that is produced by the well. Thus, EO surfactants may be useful as tracer compounds to characterize this shift from flowback to produced water.

The "Frac-t-Gram". A more detailed examination of the distribution of PEGs and LAEs can be extracted from the sample chromatograms than what is shown in Table 3. For example, Figure S2 (Supporting Information) shows the extracted ion chromatogram from the database determination of linear alkyl ethoxylates from LAE C-12 EOs to C-15 EOs for the two flowback samples, SF-1 and SF-2. These two samples have markedly different patterns of LAE-EOs. SF-1 contains the highest concentrations of C-12 ethoxylates (from EO3 to EO20) and gradually decreases with C-13 LAEs (from EO3 to EO16) and the least amount of C-14 LAEs (from EO3 to EO14) and C-15 LAEs (from EO3 to EO13).

On the other hand, SF-2 has lower concentrations of C-12 LAEs (EO3−EO10), low concentrations of C-13 LAEs (EO3−EO13), and the highest concentrations of C-14 LAEs (EO5−EO16) and C-15 LAEs (from EO11−EO15). The intensity scale is the same for the two samples, so intensities are compared in a relative, qualitative sense. The comparison of these two samples shows that they have different water chemistries that probably originated from different initial application of hydraulic fracturing fluids to the well, or perhaps, the surfactants could have undergone some removal (e.g., sorption) during the fracturing process in the deep wells, i.e. ∼10 000 feet. This comparison of the extracted ion chromatograms between samples by the database program is called a "Frac-t-Gram", which is a combination of part of the word fracturing and the suffix -gram, meaning "a written word' in ancient Greek. Its usefulness is that it gives a quick visual comparison of the distribution of PEG-EOs or LAE-EOs present in the flowback and produced water samples (see Figures S2 and S3 of the Supporting Information and the TOC graphic). The Frac-t-Gram is not part of the Agilent Mass Hunter software.

The Frac-t-Grams for the PEG-EO surfactants for SF-1, SF-2, and GF-1 are shown in Figure S3 (also the TOC figure), which shows the bimodal distribution of PEGs in sample SF-1, which was not present in samples SF-2 and GF-1. Thus, the bimodal distribution sets the SF-1 sample apart from the other two samples. The Frac-t-Grams for both the PEG-EOs and the LAE-EOs (Figures S2 and S3, Supporting Information) can be compared to generate a fingerprint for a water sample (see the TOC graphic).

Another use of the Frac-t-Gram is to compare water samples from a continuous sampling of a specific extraction well from which fluid is recovered for several days to weeks after a hydraulic fracturing event and before or during the initial stages of oil or natural gas production. In the process, the water sample changes from a flowback sample to a produced water sample. For example, two samples were collected at 3 days and 3 weeks for SF-2 and SF-3, respectively. The 3-week sample had complete removal of its LAE ethoxylate fingerprint—none were found by the database program—but it did still contain its PEG-EO signature, but with losses of the longer chain PEGs (EO-20−EO22 were not present). This result suggests that the LAE-EOs and the more hydrophobic PEGs were removed in the fracturing process (i.e., due to sorption and dilution), while the majority of the PEGs, being more hydrophilic, were still present in the produced water samples.

The database program generates much more detailed information on each of the chromatographic peaks in the Frac-t-Gram (both PEG-EOs and LAE-EOs). For example, Figure S4 in the Supporting Information shows a "snapshot" of the instrument's computer screen with detailed information on the number of compounds detected. In this example, 54 LAE-EOs were found in SF-1. If one clicks on an individual compound in the software window, then other subwindows appear with the compound formula, mass, retention times, peak areas, peak heights, mass accuracies, the different types of adducts, and different charge states. The operator is free to examine the mass spectrum, as well, to verify the detections if deemed necessary. The MassHunter software is using the csv Excel file and the "Find by Formula" tab, as described in the Experimental Section.

Finally, future work will continue to apply the use of the PEG-EO and LAE-EO databases to both flowback and produced water samples from other active drilling sites. This will give the opportunity to expand the database to different suites of PEG-EOs and LAE-EOs that may be present. Furthermore, the approach outlined here will be applied to the sulfur-containing surfactants that are also used in hydraulic fracturing fluids, i.e., the sulfonates, sulfonic acids, and ethoxysulfonates. The usefulness of fingerprinting with Frac-t-Grams will require more samples, which will hopefully become available as the energy companies continue their studies. However, as collaborations continue, as occurred in this study, flowback water, produced water, surface water, and groundwater samples will become available for detailed analysis. Finally, this method may also help the oil and gas industry to

dx.doi.org/10.1021/ac502163k | Anal. Chem. 2014, 86, 9653−9661

optimize and potentially minimize the use of surfactants in hydraulic fracturing operations.

■ ASSOCIATED CONTENT

Supporting Information

Ion chromatography method used for identification of sodium and ammonium in mobile phases, Tables S1−S6, and Figures S1−S4. This material is available free of charge via the Internet at http://pubs.acs.org.

■ AUTHOR INFORMATION

Corresponding Authors

*E.M.T.: e-mail, michael.thurman@colorado.edu; phone, 303-564-7460

*T.B.: e-mail, thomas.borch@colostate.edu; phone, 970-491-6235.

Notes

The authors declare no competing financial interest.

■ ACKNOWLEDGMENTS

The University of Colorado group acknowledges Agilent Technologies for LC/Q-TOF/MS support and Tom Evans, Yaal Lester, James Rosenblum, and Larry Zinkel, for hydraulic fracturing water samples. The Colorado State University portion of this research was supported by The Borch-Hoppess Fund for Environmental Contaminant Research. We all thank Robert B. Young for analyzing the IC data and Multi-Chem, a Halliburton Service (Houston, TX), for supplying us with commonly used surfactant standards and two flowback water samples.

■ REFERENCES

(1) Vidic, R. D.; Brantley, S. L.; Vandenbossche, J. M. *Science* **2013**, *340*, 1235009−1.

(2) Kargbo, D. M.; Wilhelm, R. G.; Campbell, D. J. *Environ. Sci. Technol.* **2010**, *44*, 5679−5684.

(3) Gies, E. The race is on to clean up hydraulic fracturing. *The New York Times*, December 4, 2012; http://www.nytimes.com/2012/12/05/business/energy-environment/race-is-on-to-clean-up-hydraulic-fracturing.html?_r=0.

(4) Jolly, D. France upholds ban on hydraulic fracturing. *The New York Times*, October 11, 2013;http://www.nytimes.com/2013/10/12/business/international/france-upholds-fracking-ban.html.

(5) Wernau, J. Bill to regulate fracking in Illinois sails through committee. *Chicago Tribune* May 21, 2013; http://articles.chicagotribune.com/2013-05-21/business/chi-bill-to-regulate-fracking-in-illinois-sails-through-committee-20130521_1_fracking-gas-drilling-tribeca-film-festival.

(6) The Safe Drinking Water Act-Public Law 93-523.

(7) The Energy Policy Act, 2005, Public Law 109-58.

(8) EPA's Study of Hydraulic Fracturing and Its Potential Impact on Drinking Water Resources; http://www2.epa.gov/hfstudy.

(9) http://www.halliburton.com/public/projects/pubsdata/Hydraulic_Fracturing/fluids_disclosure.html.

(10) List of Hydraulic Fracturing Compounds from Wikipedia; http://en.wikipedia.org/wiki/List_of_additives_for_hydraulic_fracturing.

(11) FracFocus.org; http://fracfocus.org/regulations-state.

(12) *Chemicals Used in Hydraulic Fracturing;* United States House of Representatives Committee on Energy and Commerce: Washington DC, 2011; http://democrats.energycommerce.house.gov/sites/default/files/documents/Hydraulic-Fracturing-Chemicals-2011-4-18.pdf.

(13) Stringfellow, W. T.; Domen, J. K.; Camarillo, M. K.; Sandelin, W. L.; Borglin, S. *J. Hazard. Mater.* **2014**, *275*, 37−54.

(14) Kendrick, E. *Anal. Chem.* **1963**, *35*, 2146−2154.

(15) Hughey, C. A.; Hendrickson, C. L.; Rodgers, R. P.; Marshall, A. G. *Anal. Chem.* **2001**, *73*, 4676−4681.

(16) Barrow, M. P.; Witt, M.; Headley, J. V.; Peru, K. M. *Anal. Chem.* **2010**, *82*, 3727−3795.

(17) Sleighter, R. L.; Hatcher, P. G. *J. Mass Spectrom.* **2007**, *42*, 559−574.

(18) Riley, K. E.; Brothers, E. N.; Ayers, K. B.; Merz, K. M. *J. Chem. Theory Comput.* **2005**, *1*, 546−553.

(19) Gagliardi, L. G.; Castells, C. B.; Ràfols, C.; Rosés, M.; Bosch, E. *J. Chem. Eng. Data* **2007**, *52*, 1103−1107.

(20) Lerno, L. A.; German, J. B.; Lebrilla, C. B. *Anal. Chem.* **2010**, *82*, 4236−4245.

(21) Crescenzi, C.; Di Corcia, A.; Marcomini, A.; Semperi, R. *Environ. Sci. Technol.* **1997**, *31*, 2679−2685.

(22) Ferrer, I., Furlong, E. T., Thurman, E. M. In *Liquid Chromatography/Mass Spectrometry, MS/MS and Time-of-Flight MS: Analysis of Emerging Contaminants*, Ferrer, I., Thurman, E. M., Eds.; ACS Symposium Series 850; American Chemical Society: Washington, DC, 2002; pp 376−393.

(23) Traverso-Soto, J. M.; Lara-Martin, P. A.; Leon, V. M.; Gonzalez-Mazo, E. *Talanta* **2013**, *110*, 171−179.

(24) Wyttenbach, T.; von Helden, G.; Bowers, M. T. *Int.. J. Mass Spectrom. Ion Processes* **1997**, *165/166*, 377−390.